

Quick-look outlier detection for GOCE gravity gradients

Johannes Bouman
SRON National Institute for Space Research
Sorbonnelaan 2, 3584 CA Utrecht, The Netherlands

December 20, 2004

Abstract

GOCE will be the first satellite ever to measure the second order derivatives of the Earth's gravitational potential in space. With these measurements it is possible to derive a high accuracy and resolution gravitational field if systematic errors and/or outliers have been removed to the extent possible from the data. It is necessary to detect as many outliers as possible in the data pre-processing because undetected outliers may lead to erroneous results when the data are further processed, for example in the recovery of a gravity field model. Outliers in the GOCE gravity gradients, as they are likely to occur in the real observations, will be searched for and detected in the processing step preceding gravity field analysis.

As the diagonal gravity gradients are the main gradient observables for GOCE, three methods are discussed to detect outliers in these gradients. The first is the tracelessness condition, that is, the sum of the diagonal gradients has to be zero. The second method compares GOCE gravity gradients with model or filtered gradients. Finally, along track interpolation of gravity gradient anomalies is discussed. Since the difference between an interpolated value and a measured value is large when outliers are present, along track interpolation is known to be suitable for outlier detection. The advantages and disadvantages of each method are discussed and it is shown that the final outlier detection algorithm, which is a combination of the three methods, is able to detect almost all outliers while the number of falsely detected outliers remains small.

Key words. Outliers · GOCE mission · Gradiometry · Statistical tests

1 Introduction

Outlier detection is one of the important tasks in the GOCE data pre-processing. In this paper, the focus will be on the gravity gradients (GG). The outliers themselves may point to possible instrument problems, while undetected outliers may lead to erroneous results when the data are further processed, for example in the external calibration of the gravity gradients, in the gravity field analysis or in the error assessment. It is therefore important to detect as many outliers as possible in the data pre-processing. A restriction in the context of quick-look data processing is the time required to detect outliers. The outlier detection algorithm that is implemented should have a short run-time, while the intervention by an operator should be minimal, that is, the s/w has to be fully automated.

First, the outlier detection is described in the pre-processing context. Second, several outlier detection methods are discussed and compared. Finally, the outlier detection methods are tested in a simulation study and the overall algorithm is discussed. Alternatives are discussed in, for example (Albertella et al. 2000; Bouman et al. 2004a; Kern et al. 2004; Tscherning 1991).

2 Pre-processing

Since the main goal of the GOCE mission (expected launch in August 2006) is to provide unique models of the Earth's static gravity field (ESA 1999), the GOCE gravity gradients need to be corrected for temporal gravity field variations such as tides. Furthermore, even after in-flight calibration the observations will be contaminated with stochastic and systematic errors. Systematic errors include GG scale factor errors and biases (Cesare 2002) which one tries to correct for in the external calibration step (see e.g. Bouman et al. 2004b). Also outliers in the GOCE gravity gradients need to be searched for and detected in the Level 2 pre-processing step. The steps for quick-look pre-processing are:

1. corrections for temporal gravity field variations;
2. outlier detection and correction;
3. external calibration and error assessment;
4. iteration of steps 2 and 3.

3 Outlier detection

We will consider time series of gravity gradients

$$V_{\eta\eta}(\tau_i), \quad i = 1 : m \quad (1)$$

with $\tau_i - \tau_{i-1} = 1$ s, $\eta\eta = xx, yy$ or zz and m the number of observations.

First, data snooping is discussed when a model of condition equations is used, which will be the starting point for our outlier detection. Then we will discuss the tracelessness condition which will be the baseline method for outlier detection. The comparison of measured gradient with model gradients (gradient anomalies) and the interpolation of the gradient anomalies are discussed as well.

3.1 Data snooping

Let's assume that the $m \times 1$ vector \underline{y} contains the diagonal gravity gradients which errors are normally distributed with known error variance matrix Q_y :

$$\underline{y} \sim N(E\{\underline{y}\}, Q_y) \quad (2)$$

with E the expectation operator. All single observations will be tested for outliers. The hypothesis

$$H_0 : B^T E\{\underline{y}\} = 0 \quad (3)$$

will be tested against

$$H_A : B^T E\{\underline{y}\} = c_t \nabla, \quad \nabla \neq 0 \quad (4)$$

where B^T is the condition equation matrix, $c_t = B^T c_y$ and c_y is a unit vector with 1 at row i if the i -th observations is to be tested, and ∇ is an outlier with unknown size. In the condition equation (3), the matrix B^T has b rows, the number of conditions, and it has m columns, the number of observations. It can be shown that H_0 will be rejected if, see (Teunissen 2000):

$$w < -k_\alpha \text{ or } w > k_\alpha \quad (5)$$

with

$$\underline{w} = \frac{c_t^T Q_t^{-1} \underline{t}}{\sqrt{c_t^T Q_t^{-1} c_t}} \quad (6)$$

where $\underline{t} = B^T \underline{y}$ is the vector of misclosures, $Q_t = B^T Q_y B$, and k_α is the critical value which depends on the significance level α . The random variable \underline{w} is the w-teststatistic and has a standard normal distribution under H_0 . A disadvantage of data snooping may be that it is computationally intensive. In general Q_t is a full matrix and its inverse has to be computed.

One can make two types of errors in hypothesis testing (Teunissen 2000). *Type I error*: rejection of H_0 when H_0 is true, that is, an outlier is detected, but there is no outlier; *Type II error*: acceptance of H_0 when H_0 is false, that is, an outlier goes undetected.

3.2 Tracelessness condition

The sum of the diagonal gravity gradients has to be zero which is called Laplace's equation or the tracelessness condition (Heiskanen and Moritz 1967). For observed gradients one has

$$E\{V_{xx} + V_{yy} + V_{zz}\} = 0 \quad (7)$$

and

$$Q_y = \begin{pmatrix} Q_{V_{xx}} & 0 & 0 \\ 0 & Q_{V_{yy}} & 0 \\ 0 & 0 & Q_{V_{zz}} \end{pmatrix} \quad (8)$$

under the assumption that there is no error correlation between the different gradients. One problem is that the gravity gradients suffer from systematic errors before external calibration of which biases and scale factor errors are the most important. For GG the effect of a scale factor error is the largest at a frequency of 0 Hz and also the bias is manifest at this frequency. Therefore, the median of the sum of the diagonal gradients over the time interval considered is subtracted in (7). Since the mean is more sensitive to outliers than the median, the former is not used.

The Q_t -matrix, needed in the test (6), is

$$Q_t = Q_{V_{xx}} + Q_{V_{yy}} + Q_{V_{zz}}. \quad (9)$$

If the along-track error correlation is neglected, then the $Q_{V_{\eta\eta}}$ are diagonal and the w-teststatistic becomes

$$w(i) = \frac{V_{xx}(i) + V_{yy}(i) + V_{zz}(i) - \text{median}}{\sqrt{\sigma_{V_{xx}}^2(i) + \sigma_{V_{yy}}^2(i) + \sigma_{V_{zz}}^2(i)}} \quad (10)$$

with $i = 1 : m$ and m the number of observation points. It is well known that the GOCE GG along-track error correlation is high. Nevertheless, it may be that for outlier detection one can neglect this correlation. Moreover, in the simulation study the $Q_{V_{\eta\eta}}$ matrices are taken as scaled unit matrices. If the along-track error correlation would not have been neglected, the Q_t matrix would have become full, which makes the computation of its inverse much more problematic. One could of course work with distinct patches of, for example, 50 observations neglecting the correlation between patches. However, the choice of the patch size is arbitrary and the observations within one patch would be treated differently, which leads to an incoherent test method.

The advantage of the tracelessness condition is that the signal-to-noise ratio (SNR) is very small. In fact, the SNR can not be smaller, which means that outliers that are well above the noise can be detected easily. A disadvantage is that with this method one can not discriminate between outliers in V_{xx} , V_{yy} and V_{zz} .

3.3 Gravity gradient anomalies

The idea is to predict gravity gradients in the GOCE orbit points from a global gravity field model and to compare them with the GOCE GG. The condition equation is

$$E\{V_{\eta\eta} - U_{\eta\eta}\} = 0 \quad (11)$$

with error matrix

$$Q_y = \begin{pmatrix} Q_{V_{\eta\eta}} & 0 \\ 0 & Q_{U_{\eta\eta}} \end{pmatrix} \quad (12)$$

where the error of the model gradients is described by $Q_{U_{\eta\eta}}$. Among others, this error depends on the accuracy of the global model, the omission error, attitude errors and the accuracy of the orbit.

In this case, the Q_t -matrix is

$$Q_t = Q_{V_{\eta\eta}} + Q_{U_{\eta\eta}}. \quad (13)$$

If it is assumed that Q_t is diagonal (no along-track error correlation), then the w-teststatistic becomes

$$w(i) = \frac{V_{\eta\eta}(i) - U_{\eta\eta}(i) - \text{median}}{\sqrt{\sigma_{V_{\eta\eta}}^2(i) + \sigma_{U_{\eta\eta}}^2(i)}} \quad (14)$$

for $i = 1 : m$. Also here the median is subtracted. Furthermore, in the simulation study the Q matrices are taken as scaled unit matrices.

One problem of condition (11) may be that the omission error is large, for example when a GRACE-only model is used, or that the commission error is large, for example when OSU91A is used. Thus the total σ may be large and the test has little ‘power’. However, all GG are tested separately and point wise and it is therefore an unambiguous test.

3.4 Overhauser spline interpolation

As an alternative to (11), consider the interpolation of anomalies along tracks. The interpolated gravity gradient anomaly can be compared with the ‘measured’ anomaly, $T_{\eta\eta} := V_{\eta\eta} - U_{\eta\eta} - \text{median}$, and

$$E\{T_{\eta\eta}^{int} - T_{\eta\eta}\} = 0, \quad \eta\eta = xx, yy, zz \quad (15)$$

with $T_{\eta\eta}^{int}$ the interpolated value. The error of the interpolated anomalies depends on the interpolation method, the orbit accuracy and on the errors of the observed GG. To a lesser extent also the accuracy of the model gradients $U_{\eta\eta}$ has an effect on the error. There are many possible interpolation methods but only Overhauser splines are considered (Overhauser 1968). The computations are simple and fast, while the interpolation errors are small, see (Bouman and Koop 2003). For equidistant data along track the condition equations take the form

$$y_i = \frac{2}{3}(y_{i-1} + y_{i+1}) - \frac{1}{6}(y_{i-2} + y_{i+2}). \quad (16)$$

If there are m observations, then i may take the values $3 : m - 2$. (The weights given in (Bouman and Koop 2003) are incorrect. The interpolation errors reported there become even smaller using the correct weights.)

Under the assumption that the error matrices are scaled unit matrices, the w-teststatistic may be approximated with

$$w(i) = \frac{1}{\sqrt{70}\sigma_{T_{\eta\eta}}} \sum_{k=i-2}^{i+2} a_k T_{\eta\eta}(k) \quad (17)$$

Table 1: Noise, outlier and gravity gradient anomaly ($V_{\eta\eta} - U_{\eta\eta}$) properties, values in [mE].

Small set	(86,351 pts)	V_{xx}	V_{yy}	V_{zz}
noise	mean	1443.7	-805.2	2248.9
	rms	2.2	4.4	5.7
outliers	mean	0.5	0.3	0.0
	rms	58.9	27.9	52.7
anomalies	mean	0.0	1.5	-1.5
	rms	36.4	35.3	58.9
Large set	(5,097,835 pts)	V_{xx}	V_{yy}	V_{zz}
noise	mean	0.0	0.0	0.0
	rms	10.1	2.7	10.0
outliers	mean	0.0	0.0	0.0
	rms	78.5	78.5	78.5
anomalies	mean	0.0	-0.4	0.4
	rms	37.2	35.3	60.0

Table 2: Type I error for case 1 in % (no outliers, critical value is ± 2); T – tracelessness condition, M – model gradients, S – spline interpolation, TMS – T + M or T + S.

Method	Small data set			Large data set		
	V_{xx}	V_{yy}	V_{zz}	V_{xx}	V_{yy}	V_{zz}
T	0.0	0.0	0.0	4.7	4.7	4.7
M	6.2	6.0	5.9	6.3	6.4	6.2
S	0	0	0	0	0	0
TMS	0	0	0	0.3	0.3	0.3

for $i = 3 : m - 2$, with weights $a_{i-2} = a_{i+2} = -1$, $a_{i-1} = a_{i+1} = 4$ and $a_i = -6$. ($\sum a_k^2 = 70$)

The advantage of this method is that each GG can be tested separately. A disadvantage is that several consecutive points are combined, which may hinder the identification of points with outliers (masking).

4 Simulation study

Two data sets with different characteristics were studied. One is a small data set with a length of 1 day which contains various types of outliers. The second data set has a length of 59 days and contains single and bulk outliers. These gradients allow for gravity field analysis (GFA).

The first data set used in this study consists of the diagonal gravity gradients V_{xx} , V_{yy} and V_{zz} which were simulated using EGM96 (Lemoine et al. 1998) for a 1 day orbit with a sampling rate of 1 s. Simulated, correlated noise was added to the signals, the data statistics are given in Table 1. The model gradients were generated using OSU91A (Rapp et al. 1991). The second data set used in this study also consists of the diagonal gravity gradients which were simulated using OSU91A for a 59 day orbit with a sampling rate of 1 s (over five million data points). Simulated, correlated noise was added to the signals. In this case, model gradients were generated using EGM96.

Errors other than outliers and simulated noise were not considered in this study, that is, orbit errors, omission errors, etc. are all zero.

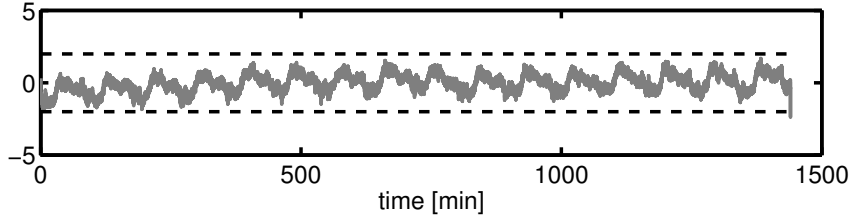


Figure 1: Test values for tracelessness condition, case 1, small data set. The dashed lines denote the critical value ± 2 .

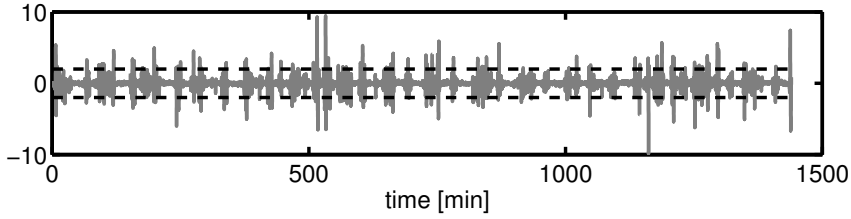


Figure 2: Test values for $V_{xx} - U_{xx}$, case 1, small data set. V_{xx} are simulated GOCE gradients, whereas U_{xx} are model gradients. Test values for V_{yy} and V_{zz} are similar to V_{xx} . The dashed lines denote the critical value ± 2 .

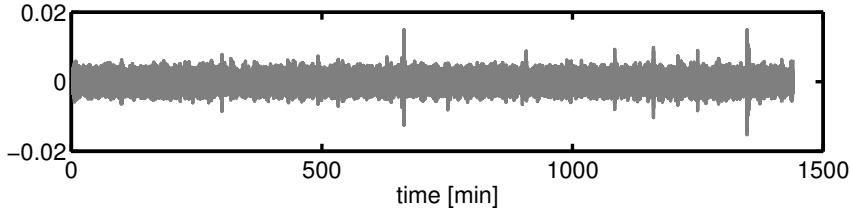


Figure 3: Test values for T_{xx} spline interpolation, case 1, small data set. Test values for T_{yy} and T_{zz} are similar to T_{xx} .

4.1 Case 1: no outliers

A first test was done that used the noisy gradients without any outliers (case 1). Fig. 1 - 3 show the w-test values for the tracelessness condition, gradient anomalies and spline interpolation respectively (small data set), while the type I error is summarised in Table 2. Given the critical value of $k = 2$, approximately 4.6% of the observations should be rejected although they are correct. For the tracelessness condition, however, the type I error is 0% for the small data set, while it is according to the expected value for the large data set. The former may be due to the error correlation between the different simulated diagonal gradients. In the small data set these errors are heavily correlated, which is neglected, whereas there is no error correlation between different gradients for the large data set. The type I error is also 0% for the spline interpolation for both data sets. Both the small and the large data sets have errors with a high spatial correlation along tracks. These long wavelength errors, however, cancel in the spline interpolation as it is a local interpolation method. This could explain the small type I error.

The model gradients have a large type I error as it is dominated by the model error, that is, the difference between EGM96 and OSU91A. The type I error is probably larger than expected because we have used a simple scaled unit matrix as error covariance matrix. Despite the some-

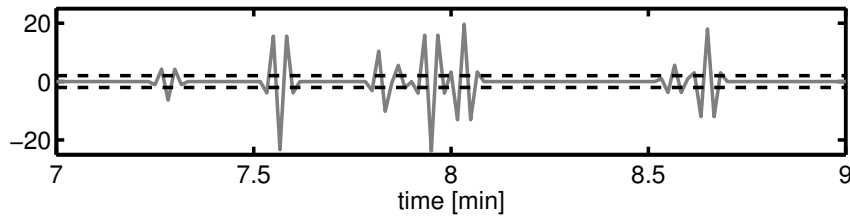


Figure 4: Test values for T_{xx} spline interpolation, case 2a. Panel zooms in on $t = 7 - 9$ min. The dashed lines denote the critical value ± 2 .

what larger type I error, model gradients may be usefull. First of all, it may be that at the time GOCE flies a more accurate gravity field model is available, which would reduce the type I error. Secondly, with the gradient anomalies one can test the individual gradients point wise. In contrast, with the trace condition one tests point wise the sum of three gradients, while with spline interpolation individual gradients are tested on an interval. Thus the three methods are complementary.

A combination of the three methods gives good results which is shown in Table 2. In this case combined means that if an outlier is detected by the tracelessness condition and if it is confirmed by a 2nd method, an outlier is flagged. The type I error is close to zero for all gradients.

4.2 Case 2: outliers on V_{xx} , V_{yy} and V_{zz}

To the small data set outliers with the following characteristics were added (case 2a): A total of 3891 randomly distributed single outliers for V_{xx} with an absolute size varying between 0.07 E and 0.1 E; An offset of 0.5 E during one minute ($\tau = 20 - 79$ s) for V_{yy} and a bulk of outliers during six minutes ($\tau = 50000 - 50359$ s) with an absolute size varying between 0.07 E and 0.1 E; A total of 994 ‘twangs’, randomly distributed, for V_{zz} , that is, an outlier at $\tau = \tau_i$ is followed by an outlier with opposite sign and of the same size at $\tau = \tau_{i+1}$. In total $2 * 994 = 1988$ outliers with absolute size between 0.07 E and 0.1 E. For the large data set 83153 outliers were added to all three gradients with an absolute size varying between 0.05 E and 1.8051 E (case 2b). The outliers were randomly distributed single outliers as well as bulk outliers, see Table 1 for data statistics.

The tracelessness condition detects almost all outliers, see Table 3 and 4. If we would use the tracelessness condition only and no other method then one cannot discriminate which diagonal GG contains an outlier and all three GG would be flagged if one of them does contain an outlier, which leads to large type I errors.

Most of the outliers are detected when gradient anomalies are used, but the type II error can be relatively large. Only 3/4 of the V_{zz} outliers of the small data set are detected for example, which is caused by the larger GOCE GG error and the larger difference between the ‘true’ GG and the model GG. The type I error is of course at the level of case 1, see Table 3 and 4. As an alternative to model gradients, one could also filter the GOCE GG with outliers and use these as ‘model gradients’. A 2nd order low-pass Butterworth filter has been used with a cut-off frequency of 0.2 Hz. Except for the gradients with an offset, the method with filtered gradients detects most of the outliers. The type I error can be large because low-pass filtering not only reduces the size of the outliers, but redistributes their power over neighbouring points as well. An offset tends to cancel and is therefore hard to detect with filtered gradients.

With spline interpolation the major part of the V_{xx} outliers (case 2a) is detected, but many valid observations are flagged as outliers, see Table 3. The type I error is large because one outlier may affect five consecutive w-test values, see Fig. 4. As an alternative to this outlier detection in one step, one could use an iterative procedure, that is, reject the global maximum, replace the

Table 3: *Detected outliers for case 2a in % (outliers on all three diagonal gradients, small data set, critical value is ± 2); T – tracelessness condition, M – model gradients, F – filtered gradients, S – spline interpolation, TMS – T + M or T + S, TFS – T + F or T + S.*

Method	V_{xx}		V_{yy}		V_{zz}	
	correct	type I	correct	type I	correct	type I
T	99.9	2.6	99.8	6.7	99.9	4.8
M	93.6	5.9	92.6	6.0	76.9	5.8
F	99.8	23.5	84.5	0.0	100	2.2
S	98.9	11.6	77.6	0.0	99.5	2.0
TMS	99.8	0.5	98.6	0.4	99.7	0.4
TFS	99.9	0.7	87.1	0	99.9	0.1

Table 4: *Detected outliers for case 2b in % (outliers on all three diagonal gradients, large data set, critical value is ± 2); T – tracelessness condition, M – model gradients, F – filtered gradients, S – spline interpolation, TMS – T + M or T + S, TFS – T + F or T + S.*

Method	V_{xx}		V_{yy}		V_{zz}	
	correct	type I	correct	type I	correct	type I
T	99.8	7.7	99.9	7.7	99.9	7.7
M	96.8	5.9	97.5	6.2	92.3	5.9
F	99.0	5.6	99.7	10.5	98.9	5.6
S	86.8	2.2	98.6	4.7	86.8	2.2
TMS	97.7	0.6	99.8	0.8	94.6	0.6
TFS	99.6	0.4	99.9	0.8	99.6	0.4

associated observation with the interpolated value, find next global maximum, etc. The iterative procedure was implemented and tested, and the type I error decreased significantly. However, also the number of detected outliers decreased, which has a negative effect on the combination solution as well. Therefore, the iterative procedure is abandoned. The spline interpolation method detects most of the bulk outliers, but is unable to detect the offset, see Table 3. An offset cancels using spline interpolation and cannot be detected directly. The type I error is small in this case because the w-test ‘side lobes’ drown in the bulk outliers. The results of the large data set (case 2b) suggest that the larger the GG noise the smaller the number of detected outliers. The GG V_{xx} and V_{zz} have a higher noise level than V_{yy} , while the number of detected outliers is the largest for the latter.

The last two rows of Table 3 and 4 show that a combination of three methods yields excellent results. An outlier is flagged if the tracelessness condition is confirmed by one of two methods. In general the method with model gradients detects less outliers than the method with filtered gradients. However, the latter is less suited to detect an offset. For a critical value of 2, about 99% of the outliers are detected, while the type I error is small, below 1%. The expected type I error is 4.6% which is much larger. This is likely due to the combination of the three methods.

Finally, Fig. 5 shows the gravity field anomaly differences between OSU91A and a quick-look GFA solution up to degree and order 250. As input the TFS cleaned GG were used (case 2b). The rms difference, excluding polar caps of 10° , is 9.8 mGal, which is somewhat larger than the difference when gradients without outliers are used in the GFA (6.7 mGal). When the TFS cleaned GG are used with an additional outlier search in the GFA, 100% of the outliers are detected and the rms gravity anomaly difference is only 6.9 mGal, see also (Bouman et al. 2004a).

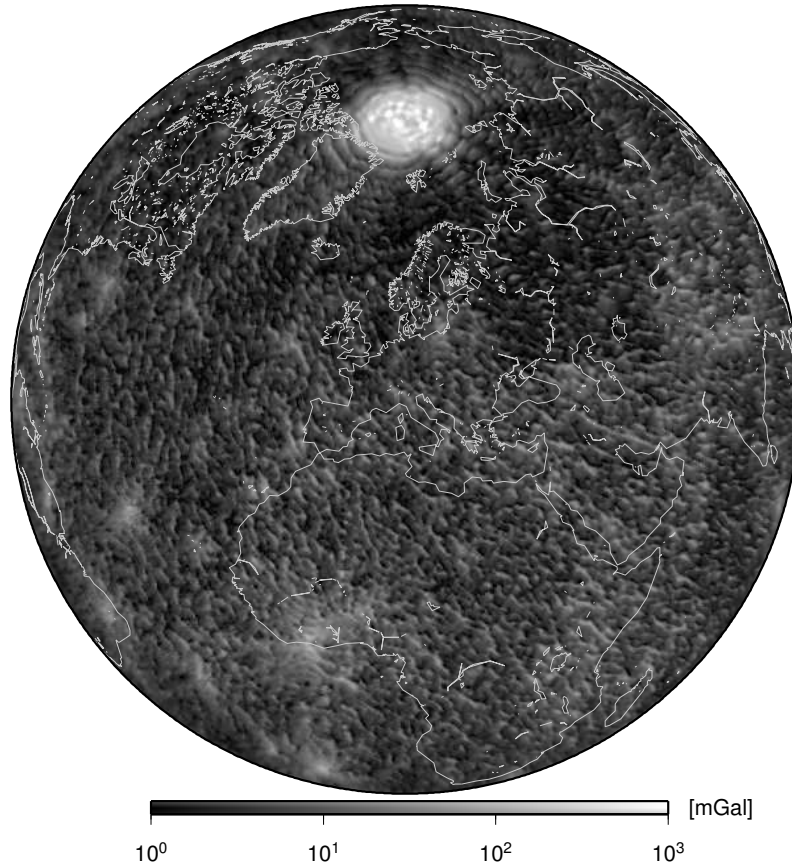


Figure 5: *Gravity anomaly differences OSU91A – QL-GFA (log scale), pre-processing outlier detection using TFS.*

5 Conclusions and outlook

The tracelessness condition is the baseline method for the quick-look outlier detection algorithm studied here. If an outlier is detected by this method and if it is confirmed by either model (or filtered) gradients and/or by spline interpolation, then an outlier is flagged. Although the individual methods have their disadvantages, their combination yields high outlier detection rates and only a small number of falsely detected outliers. The w-test, which was used, explicitly accounts for the GG errors. However, to obtain a manageable solution, the error correlations were neglected and it was even assumed that the error matrices are scaled unit matrices. Despite the heavy error correlation, outliers can be very well detected. It therefore seems that the simplifications do little harm.

To further improve the performance, the spline interpolation may be replaced by, for example, least-squares prediction. The outlier detection results may also improve by taking the spatial correlation between the observables into account using least-squares collocation (LSC), see (Tscherning 1991). It may be that the turn-around time of the current GRAVSOFTE implementation of LSC (Tscherning 1974) is acceptable for operational use. This needs, however, to be studied. Future simulation studies should also include the V_{xy} , V_{xz} and V_{yz} gradients. In addition, more realistic GOCE error characteristics should be used, and other errors, such as orbit errors or attitude quaternion errors, should be accounted for.

6 Acknowledgements

This study was performed in the framework of the ESA-project GOCE High-level Processing Facility (GOCE HPF, Main Contract No. 18308/04/NL/MM). Michael Kern computed the QL-GFA solutions and provided the GFA figure. All this is gratefully acknowledged.

References

- Albertella A, Migliaccio F, Sansò F, Tscherning CC (2000) Scientific data production quality assessment using local space-wise pre-processing. In H. Sünnkel, editor, From Eötvös to mGal, Final Report. ESA/ESTEC contract no. 13392/98/NL/GD. European Space Agency, Noordwijk
- Bouman J, Kern M, Koop R, Pail R, Haagmans R, Preimesberger T (2004a) Comparison of outlier detection algorithms for GOCE gravity gradients. Paper presented at the IAG Porto meeting (GGSM2004)
- Bouman J, Koop R (2003) Error assessment of GOCE SGG data using along track interpolation. *Advances in Geosciences*, 1:27-32
- Bouman J, Koop R, Tscherning CC, Visser P (2004b) Calibration of GOCE SGG data using high-low SST, terrestrial gravity data and global gravity field models. *Journal of Geodesy*, 78, DOI 10.1007/s00190-004-0382-5
- Cesare S (2002) Performance requirements and budgets for the gradiometric mission. Issue 2 GO-TN-AI-0027, Preliminary Design Review, Alenia, Turin
- ESA (1999) Gravity field and steady-state ocean circulation mission. Reports for mission selection. The four candidate Earth explorer core missions. ESA SP-1233(1). European Space Agency, Noordwijk
- Heiskanen W, Moritz H (1967) *Physical Geodesy*. W.H. Freeman and Company, San Francisco
- Kern M, Preimesberger T, Allesch M, Pail R, Bouman J, Koop R (2004) Outlier detection algorithms and their performance in GOCE gravity field processing. Accepted for publication in *Journal of Geodesy*
- Lemoine F, Kenyon S, Factor J, Trimmer R, Pavlis N, Chinn D, Cox C, Klosko S, Luthcke S, Torrence M, Wang Y, Williamson R, Pavlis E, Rapp R, Olson T (1998) The development of the joint NASA GSFC and the National Imagery and Mapping Agency (NIMA) geopotential model EGM96. TP 1998-206861, NASA Goddard Space Flight Center, Greenbelt
- Overhauser A (1968) Analytic definition of curves and surfaces by parabolic blending. Techn. Report No. SL68-40, Scientific Research Staff Publication, Ford Motor Company, Detroit
- Rapp R, Wang Y, Pavlis N (1991) The Ohio State 1991 geopotential and sea surface topography harmonic coefficient models. Rep 410, Department of Geodetic Science and Surveying, The Ohio State University, Columbus
- Teunissen P (2000) *Testing theory*. Series on Mathematical Geodesy and Positioning 2. Delft University Press, Delft
- Tscherning CC (1974) A FORTAN IV program for the determination of the anomalous potential using stepwise least squares collocation. Rep 225, Department of Geodetic Science and Surveying, The Ohio State University, Columbus
- Tscherning CC (1991) The use of optimal estimation for gross-error detection in databases of spatially correlated data. *Bulletin d'Information*, no. 68, 79-89, BGI